IOP Publishing

An Introduction to Plasma Physics and its Space Applications, Volume 2

Basic equations and applications

Luis Conde

Chapter 6

Introduction to plasma propulsion in space

Plasma thrusters are nowadays one of the more relevant applications of plasma physics in space technology and are used for in-space propulsion. The electric power is employed to accelerate a plasma stream or the propellant mass up to exhaust velocities one or two orders of magnitude faster than those delivered by conventional chemical propulsion. This performance drastically reduces the amount of fuel needed for a given maneuver, allowing longer mission times and heavier payloads. In this chapter we discuss the basics of electric propulsion in space and introduce some relevant plasma thruster technologies.

Plasma thrusters are used for in-space propulsion of spacecraft due to a combination of practical and economic reasons. The electric power is employed in these propulsive systems to accelerate the propellant up to exhaust velocities one or two orders of magnitude faster than those achieved in conventional chemical propulsion. Hence, the Tsiolkovsky or rocket equation (see section 6.2 and figure 6.2) shows the amount of propellant necessary for satellite maneuvers is consequently reduced. The optimal use of on-board fuel available is critical since it determines relevant issues such as the satellite mass, its size, etc. Therefore, significant propellant weight savings allow longer mission times and heavier payloads.

The rationale is to foster the economic competitiveness of satellite systems since additional services can be made available using heavier payloads. Additionally, electric thrusters are today the only propulsion technology available for some deep space missions. Today, hundreds of different electric thrusters have been tested and successfully used for orbit corrections as well as in deep-space scientific missions [1].

6.1 Basic orbital maneuvers

Nowadays, the main users of plasma thrusters commercially available are the large telecommunication satellites operated in a circular geostationary orbit (GEO; orbit altitude 35 786 km). The amount of propellant that can be made available on board is critical as they need orbit transfers and/or maneuvers along the long operational

doi:10.1088/978-0-7503-3543-0ch6

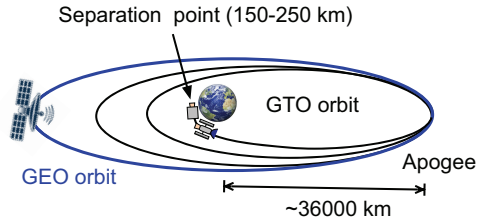

Figure 6.1. Schematic representation of the orbit transfer process of a geostationary satellite.

Table 6.1. Typical values of Δv in equation (6.3) for different maneuvers and orbit transfers from reference [3].

Maneuver	Δv (m s^{-1}) per year
Drag compensation	30
Station keeping GEO	50
Orbit transfer	**Δv (km s^{-1})**
Earth-LEO	9.7
LEO-GEO	4.3
GTO-GEO	1.5
Interplanetary	**Δv (km s^{-1})**
Nearby planets	5–8
Far planets	10–15

life of these satellites. The equatorial GEO orbit is reached by a sequence of different propellant-consuming orbital maneuvers and is schematically shown in figure 6.1, where the satellite speed $\Delta v = v_f - v_i$ changes when the thruster is fired. Reference values of Δv for orbit transfers and satellite maneuvers are in table 6.1.

In first place, these satellites describe an elliptical geosynchronous transfer orbit (GTO) after its separation from the third stage of the launch rocket. To move the satellite to a quasi-circular orbit on the Earth's equatorial plane, a thrust of about 400–500 N is applied at its apogee that increases in $\Delta v = 1.5$ km s^{-1} its speed. This transfer process from GTO to GEO orbit where the satellite motion plane with respect to the equator is also corrected, usually takes time and several thruster firings. This basic scheme is modified by a number of specific details, such as the latitude of the launch site, the maximum thrust delivered by the launcher rocket, the inclination of its initial GTO orbit with respect to the Earth's equatorial plane, etc.

The orbital drag caused by the high altitude atmospheric gases is negligible at GEO orbit. However, small perturbations in the orbital motion of satellites are produced by the lunar and solar gravitational interactions and/or the effects of the irregular distribution of Earth's mass. Hence, satellite thrusters are fired on a daily

basis to deliver 80–100 mN to compensate these perturbations during the 15–20 years duration of its mission. These maneuvers are currently denominated north–south (NSSK) and east–west (EWSK) *station keeping* and are crucial for telecommunication satellites since their uplink and downlink high gain antennas must point along precise directions [2].

Eventual collisions with other objects in orbit also require additional propellant consumption and more thrust is applied at the end of the satellite operational lifetime, since there are a limited number of slots (~400 satellites) available in GEO orbit. To avoid its eventual return to Earth's atmosphere, the satellite velocity is usually incremented in $\Delta v = 3.0$ m s^{-1} to raise its altitude about 300 km up into a graveyard orbit. This maneuver is intended to mitigate the proliferation of debris at lower altitudes [2].

Similarly, the reduced propellant available on-board also limits the operational life of GPS systems, operating in medium Earth orbits (MEO, altitudes from below 36 000 km down to 2000 km). Their precise and synchronized motions also require periodic thruster firings for orbit corrections as well as for the end-of-life satellite retirement.

Furthermore, new constellations of interconnected small satellites (100–700 kg) intended for interactive television and planetary Internet coverage are being deployed in low Earth orbit (LEO, altitudes from 160 to 2000 km). Their long-term interaction with the high altitude atmosphere is not negligible and they need to be continuously operated to compensate the orbital drag force. The size and weight of these satellites are an issue for the stowage of fuel required for orbital maneuvers and also the final satellite disposal. Conventional chemical thrusters are not an option in this case and electric propulsion is the only available technology so far.

We can conclude that service time of expensive satellites in Earth's orbit is directly related with the amount of fuel that can be stowed on board. The acceleration of charged particles by electric fields is an attractive idea, as the Tsiolkovsky equation shows that important reductions can achieved increasing the exhaust velocity of the propellant. Plasma thrusters make use of different physical mechanisms to accelerate the ejected flow of particles up to higher speeds than conventional chemical propulsion.

6.2 The Tsiolkovsky equation

The ejected propellant mass provides thrust to the spacecraft and the Tsiolkovsky or rocket equation describes the relationship between its velocity and the mass of the system. Momentum conservation (see chapter 2 of reference [4]) gives the thrust that is delivered by the mass of propellant $m_p(t)$ ejected with constant speed v_{ex} with respect to the spacecraft frame of reference as,

$$F = -\frac{d}{dt}(m_p\, v_{ex}) = -v_{ex}\,\frac{dm_p}{dt} = -v_{ex}\,\dot{m}_p$$

where $\dot{m}_p$ is also constant in time. The total mass of the vehicle is $m(t) = m_p(t) + m_f$ the sum of the propellant plus the final delivered mass m_f in the maneuver which is fixed.

Since $\dot{m}_p = m_{po}/\tau_b$ where τ_b is the burning time at a constant rate, we have $\dot{m} = \dot{m}_p$ and the equation of motion for the spacecraft with speed $v(t)$ is,

$$m\,\frac{dv}{dt} = -\,v_{ex}\,\frac{dm}{dt} \quad \text{then,} \quad \int_{v_{si}}^{v_f} dv = -v_{ex}\int_{m_f+m_{po}}^{m_f}\frac{dm}{m}$$

Here $m_o = m_f + m_{po}$ is the initial mass of the spacecraft and writing $\Delta v = v_f - v_i$ we have,

$$\frac{\Delta v}{v_{ex}} = \ln\left(\frac{m_{po}+m_f}{m_f}\right) \text{ or equivalently, } \Delta v = I_{sp}\,g_o\,\ln\left(1+\frac{m_{po}}{m_f}\right) \tag{6.1}$$

The last equation relates the increment Δv of satellite speed as required for the maneuver with the *specific impulse* $I_{sp} = v_{ex}/g_o$ where g_o is the standard Earth's gravity.

This last magnitude can also be understood as the ratio between the thrust delivered F and the weight of consumed propellant per time unit as,

$$I_{sp} = \frac{F}{\dot{m}_p\,g_o}$$

and is used to compare the performance of thrusters. Equation (6.1) can be cast as,

$$\exp\left(\frac{\Delta v}{v_{ex}}\right) = \frac{m_o}{m_f} = \frac{m_o}{m_o - m_{po}} \tag{6.2}$$

The decreasing ratio between the initial mass of the spacecraft $m_o = m_f + m_{po}$ and the mass of propellant m_{po} required for the increment Δv is,

$$\frac{m_{po}}{m_o} = 1 - e^{-\Delta v/v_{ex}} \tag{6.3}$$

and is represented in figure 6.2(a) as a function of the exhaust propellant speed.

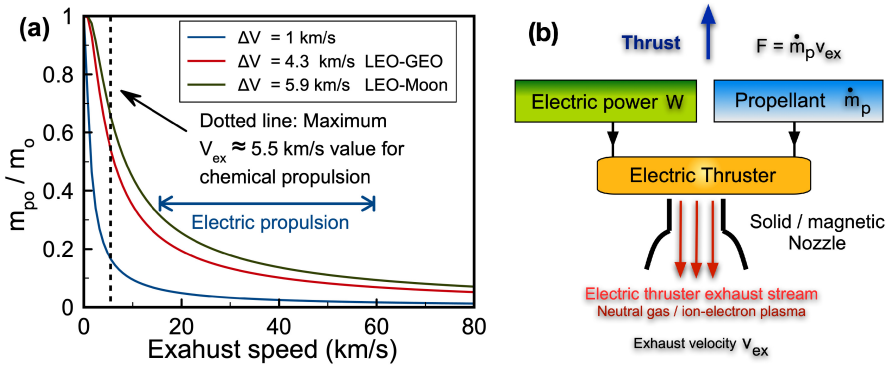

Figure 6.2. (a) The calculations of the ratio m_{po}/m_o as a function of the exhaust propellant velocity v_{ex} using the Tsiolkovsky equation (6.3) for typical values of Δv of table 6.1. The basic scheme of an electric thruster is in (b) where $\dot{m}_p$ is the propellant mass flow rate with exhaust speed v_{ex} and W is the electric power consumption.

6.3 Thrust and specific impulse

Rocket engines operate according to the principle of action and reaction where the gas exhaust speed v_{ex} is crucial for momentum transfer. The thrust is essentially delivered by the *momentum thrust* term $F = \dot{m}_p\, v_{ex}$ as the low ambient pressures in space make the *pressure thrust* negligible [4]. Under ideal conditions equation (6.1) relates the ratio m_{po}/m_f between the mass of fuel m_{po} needed to increase in $\Delta v = v_f - v_i$ the velocity of a satellite with final mass m_f (dry mass) as,

$$\frac{m_{po}}{m_f} = e^{\Delta v/v_{ex}} - 1 \tag{6.4}$$

The integration of the thrust force $F(t)$ over the burning time t_b gives the *total impulse*,

$$I_t = \int_o^{\tau_b} F(t)\, dt$$

and for constant thrust reduces to $I_t = F \times \tau_b$. The *specific impulse* I_{sp} is the *total impulse per unit weight* of propellant as,

$$I_{sp} = \frac{\displaystyle\int_o^{\tau_b} F(t)\, dt}{g_o \displaystyle\int_o^{\tau_b} \dot{m}_p(t)\, dt} = \frac{I_t}{m_p\, g_o}$$

where g_o is the standard Earth's gravity. For constant thrust F and mass flow $\dot{m}_p$,

$$I_{sp} = \frac{I_t}{m_p\, g_o} = \frac{F \times \tau_b}{\dot{m}_p \times \tau_b \times g_o} = \frac{F}{\dot{m}_p\, g_o}$$

and using $F = \dot{m}_p\, v_{ex}$ we have also $I_{sp} = v_{ex}/g_o$. Then, I_{sp} represents the *thrust delivered by the weight of propellant consumed by time unit* and measures the efficiency of the propulsive system.

Table 6.2 shows the typical values of thrust F, burning time τ_b and specific impulse for different conventional chemical thrusters. In figure 6.2(a) is represented the ratio m_{po}/m_o given by equation (6.3) against the exhaust speed v_{ex} for different v values of table 6.1.

Table 6.2. Performance data and standard propellants employed by conventional chemical thrusters from reference [3]. The typical burning time τ_b is indicated in minutes (m), hours (h) or seconds (s).

Thruster type	I_{sp}(s)	F(N)	τ_b(s)	Fuel
Cold gas	50	0.1–100	~m	N_2, ammonia
Liquid	200	1–500	~h	Hydrazine
Liquid	300–400	10^6	~m	$LO_2 + H_2$, kerosene
Solid	250	10^7	100 s	Powder (Al, Mg, Zn, S)

Cold nitrogen or ammonia gases ejected at low speeds (~0.49 km s^{-1}) are employed for low thrust maneuvers. Higher yields (up to 10^6–10^7) are delivered by mixtures of reactive liquids or solid chemicals producing hot gases with typical velocities in the range 2–4 km s^{-1}. For conventional chemical propulsion systems (such as those of table 6.2) the maximum propellant exhaust velocity that can be achieved is $v_{ex} \lesssim 5.5$ km s^{-1}, since it is limited by the energy produced by chemical reactions [4].

This upper bound for v_{ex} is indicated in figure 6.2(a) by the vertical dotted line and the ratio m_{po}/m_o decreases dramatically as the propellant exhaust velocity is increased. For example, the Space Shuttle main engines deliver hot gases with $v_{ex} \sim 4.4$ km s^{-1} and for a GTO-GEO transfer ($\Delta v = 1.5$ km s^{-1}) we obtain $m_{po}/m_o = 0.405$ which gives $m_{po} = 405$ kg for a 1000 kg satellite. Increasing $v_{ex} \sim 20$ km s^{-1} this calculation gives $m_{po}/m_o = 0.078$ reducing to $m_p = 78$ kg the weight of fuel.

The specific impulse in table 6.2 characterizes the efficiency of each propulsive system. Propellants based on liquid oxygen have a high I_{sp} as they deliver high thrust with low mass fuel consumption. In contrast, $I_{sp} = v_{ex}/g_o$ is about ten times lower for cold gas thrusters as they give much lower thrust for equal propellant weight. The underlying physical basis is the high exhaust speed v_{ex} achieved in chemically reactive liquid mixtures compared with those of cold gas expansion in a nozzle.

Increasing the specific impulse and/or the thrust delivered leads to reductions in the required propellant weight that have a direct impact in the satellite design, allowing heavier payload masses m_f and longer operational time in orbit. New technologies that increase the propellant exhaust speed have a direct impact in the economic competitiveness of satellite systems.

6.4 Electric propulsion principles

The thrust $F = \dot{m}_p\, v_{ex}$ delivered by a propulsive system is achieved by the transformation of energy (chemical, electric power, etc) into kinetic energy power [4],

$$P_b = \frac{dE_{kin}}{dt} = \frac{1}{2}\dot{m}_p\, v_{ex}^2 = \frac{F^2}{2\,\dot{m}_p} \tag{6.5}$$

of the gas, liquid or solid propellant substance.

Achieving high values of P_b in equation (6.5) in conventional chemical thrusters basically depends on the nature of the propellant substance and requires high mass flow rates $\dot{m}_p$ and/or elevated gas temperatures T. The kinetic energy power P_b comes from the transformation of thermal energy of molecules of mass m_a into a gas stream of $v_{ch} \sim \sqrt{T/m_a}$ exhaust velocity using a solid nozzle.

The in-space electric propulsion systems make use of physical processes involving electric power to increment the exhaust velocity of a plasma flow and/or to heat a gas stream. These engines operate in a high vacuum environment and the diagram of figure 6.2(b) shows schematically the basic elements of an EP system. The central block symbolizes an idealized electric engine that delivers a $F = \dot{m}_p\, v_{ex}$ thrust by transforming the electric power W into the kinetic energy power (6.5).

To this aim the electric energy is transformed into gas thermal energy raising its temperature by collisions of charged particles with neutral atoms and/or the propellant is directly heated. The thrust is delivered along a fixed direction by the hot gas exhaust expansion in a conventional solid nozzle.

Alternatively, propellant molecules can be ionized and ions of mass m_i accelerated to supersonic velocities $v_{ex} \sim \sqrt{2\, e\, \phi/m_i}$ by externally applied and/or self-consistent electric potential ϕ. The resulting ion-electron *plasma stream* that can also be focused on the direction of thrust using electrically biased electrodes and/or along the field lines of *magnetic nozzles*. No solid walls can be used in this case since ions and electrons impacting solid surfaces can recombine and/or produce additional charged particles as discussed in section 6.4.

In both cases the propellant exhaust speed is essentially independent of its chemical nature, contrary to the conventional thrusters of table 6.2. The typical exhaust velocity range of electric propulsion systems is indicated by an arrow in figure 6.2(a).

The specific performances of some electric thrusters are in table 6.3, and can be compared with those of table 6.2 for conventional chemical propulsion. The EP systems are characterized by high specific impulses $I_{sp} = v_{ex}/g_o$ and low thrusts F, whereas conventional propulsion has lower I_{sp} but delivers higher thrusts. The specific impulses in table 6.2 are below $I_{sp} = 560$ s that gives the maximum speed of $v_{ex} \sim 5.5$ km s^{-1} in figure 6.2(a). The I_{sp} values are much higher for most electric thrusters in table 6.4 reflecting the larger achievable exhaust speeds of the propellant.

A simple calculation shows the limited thrust delivered with EP systems, as high electric power and currents are required to obtain significant impulses. Under ideal

Table 6.3. Performance data and standard propellant of several types of electrical thrusters based on references [3, 5, 6]. The burning time t_b is indicated in hours (h) or is not available (n/a). The acronyms are: ECR, electron cyclotron resonance thruster; HEMPT, highly efficient multistage plasma thruster and MPD magnetoplasmadynamic thruster.

Thruster	I_{sp}(s)	Thrust (N)	Power (kW)	τ_b(s)	Propellant
Electrothermal					
Resistojet	100–300	0.2	0.1–1	~h	N_2, hydrazine, Xe
Arcjet	500	0.1	1	1000h	Hydrazine, ammonia
Helicon	~500	0.001	0.1	n/a	Ar, Kr
ECR	1000	0.001	0.03	n/a	Xe
Electrostatic					
Gridded ion engine	3000	10^{-3}–0.1	0.1–5	30 000 h	Xe
Hall thruster	1500	0.01–1	0.2–20	10 000h	Xe
HEMPT	1500–3000	0.04–0.1	5–6	9000 h	Xe
Electromagnetic					
MPD thruster	1000–10 000	0.5–50	100–10^3	1000 h	Ar, H_2, Li

Table 6.4. The characteristics of electric power sources employed in space from reference [3] where RTG is the radioisotope thermoelectric generator. The constant α_w is called *specific power* of the equipment.

	Solar panels	Batteries	RTG
Power (kW)	1–15	0.1–100	0.1–1
Efficiency η_e (%)	20–30	90	8
α_w (W kg^{-1})	150–300	100–1000	5

conditions, the maximum thrust values given by the ion beam current I_b of single charged ions accelerated by the electric potential drop ϕ can be estimated as,

$$F = \sqrt{\frac{2\,m_i}{e}}\; I_b\,\sqrt{\phi} \tag{6.6}$$

where m_i is the ion mass and e the elementary charge. The acceleration of $I_b = 1.5$ A current of xenon ions through a 1.5 kV voltage drop requires 2.25 kW of electric power and only 95.9 mN are obtained using equation (6.6). This value drops to 54.6 mN for argon gas because of its lower atomic mass. Therefore, to achieve impulses as low as 0.01 N would require space systems to cope with high voltages and large currents.

The electric energy that can be made available in the satellite and the weight of the power supply source are two criteria of relevance for EP systems. Table 6.4 shows the characteristics of electric power sources usually employed in spacecraft. The efficiency η_e for a solar panel is the fraction of sunlight energy[1] converted into electricity which is below η_e for batteries. Both are used in combination to power satellites in Earth orbit, whereas radioisotope thermoelectric sources (RTG) are less efficient and mainly used in deep space exploration.

In conventional chemical propulsion the weight of propellant decreases in time, whereas in EP systems the energy source remains constant, so its advantages can be outweighed by the large mass of the electric power equipment required. The *specific power* coefficient α_w in table 6.4 is the estimated rate between the output power delivered in watts and the average weight of the power supply in kilograms. For a typical $\alpha_w = 225$ W kg^{-1} value and 2.25 kW we need 10 kg of power equipment to deliver 95.9 mN as in the above example. As a consequence, applications of in-space electric propulsion are restricted to low thrust until new advances in electric power technology improve the basic data of table 6.4.

Chemical thrusters have burning times τ_b from minutes to one hour in table 6.2, whereas most electric propulsion systems in table 6.3 have τ_b between 10 000 hours (427 days) and 30 000 hours. This last figure represents more than three years of continuous operation and therefore the *total impulse* $I_t = F \times \tau_b$ delivered can be comparable to the thrusters of table 6.2. Therefore, electric propulsion can be

[1] It is usually estimated as 1360 W m^{-2} for Earth orbit.

advantageous for long time maneuvers, as the amount of propellant required is much lower.

For example, the 400 N hydrazine monopropellant thruster used by the Ariane 5 G upper stage consumes 300 kg of propellant in 850 seconds to deliver a maximum impulse $I_t = 1.88 \times 10^3$ N. The Hall effect thruster in table 6.3 reaches this total impulse in 56 hours using much lower propellant weight.

6.4.1 Efficiencies

The kinetic energy P_b per time unit delivered to the ion beam of figure 6.2(b) by the thruster is the *beam* or *kinetic power* introduced in equation (6.5),

$$P_b = \frac{1}{2} F \times v_{ex} = \frac{F^2}{2\,\dot{m}_p}$$

When plasma acceleration is the working principle of a thruster, not all particles in the propellant gas are ionized and neutral atoms do not significantly contribute to either P_b or the thrust F. We can introduce the *mass utilization efficiency* as the ratio,

$$\eta_m = \frac{\dot{m}_i}{\dot{m}_p} \leqslant 1$$

which measures the efficiency of the propellant ionization. This parameter is $\eta_m = 1$ in the limit cases of fully ionized gas or when the thrust is not produced by charged particle acceleration. As the propellant mass rate m_p is usually simpler to control than $\dot{m}_i$ we have,

$$F = \dot{m}_i\, v_{ex} = \eta_m\, \dot{m}_p\, v_{ex} \quad \text{and,} \quad P_b = \frac{F^2}{2\,\eta_m\,\dot{m}_p}$$

and the specific impulse can be also corrected since,

$$I_{sp} = \frac{F}{\dot{m}_p\, g_o} = \eta_m \frac{v_{ex}}{g_o} \tag{6.7}$$

The electrical efficiency of a thruster can be characterized by the *thrust* or *electrical efficiency* parameter [3, 7],

$$\eta_e = \frac{P_b}{W_T} < 1$$

where W_T is the total electrical input power of the thruster. This ratio measures the efficiency in the conversion of electric power in propellant kinetic energy and we have $\eta_e < 1$ since this conversion is not perfect. We can write,

$$\frac{F}{W_T} = \eta_e \times \frac{F}{P_b} = \eta_e \times \frac{2}{v_{ex}}$$

and using $v_{ex} = I_{sp} \times g_o/\eta_m$

$$\frac{F}{W_T} = \eta_e\, \eta_m \times \frac{2}{I_{sp}\, g_o} \tag{6.8}$$

We can introduce a *total efficiency* $\eta_T = \eta_m \times \eta_e$. In figure 6.3 are represented the values of equation (6.8) as a function of the specific impulse I_{sp} for different rations η_T together with the actual characteristics of different propulsive systems. Equation (6.8) can be used to relate the electric power required by the thrusters of figure 6.3. For example a 100 mN impulse from an HET thruster with $\eta_T = 0.5$ and $I_{sp} \simeq 2000$ s requires about 2 kW power.

The solid red line of $\eta_T = 100\%$ in figure 6.3 indicates the *maximum ideal efficiency* when all propellant neutral gas is fully ionized ($\eta_m = 1$) and additionally all available electric power W_T is transformed into kinetic energy ($\eta_e = 1$) of ions in the plasma jet. The solid lines below correspond to the decreasing efficiencies in equation (6.8). At the left of the dotted vertical line, which marks limit ($I_{sp} \simeq 560$ s) lies the classical chemical propulsion as well as arcjets and resistojets. Most commercial electric thrusters (GIE and HET) have specific impulses over 1000 s and efficiencies in the order of $\eta_T \sim 50\%$ approximately.

6.5 Modified Tsiolkovsky equation

Next, we will consider the corrections introduced by the weight of electric power equipment in masses ratio in the Tsiolkovsky equation. The propellant consumption m_{po} along the burning time τ_b is,

$$m_{po} = \dot{m}_p \times \tau_b = \frac{\dot{m}_i}{\eta_m} \times \tau_b = \frac{\tau_b}{\eta_m} \times \frac{F}{v_{ex}}$$

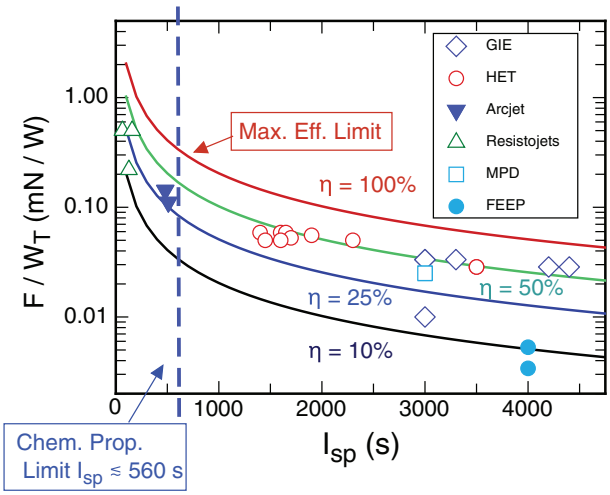

Figure 6.3. Equation (6.8) for different total efficiency rates η_T as a function of the specific impulse I_{sp}. The symbols corresponds to actual values of commercial electric thrusters of table 6.5.

replacing v_{ex} using equation (6.7),

$$m_{po} = \frac{F\ \tau_b}{g_o} \times \frac{1}{I_{sp}}$$

The amount of fuel m_{po} decreases with I_{sp}, however, we need to consider also the weight of the electric power equipment that is constant in time. This mass can be considered approximately proportional to the electrical power W supplied, $m_w = \alpha_w\ W$ where the constant α_w is called *specific power* and its typical values are in table 6.4. We can write,

$$m_w = \alpha_w\ W = \alpha \times \frac{P_b}{\eta_e} = \frac{\alpha_w}{2\ \eta_e} F \times v_{ex}$$

where the electric power W is transformed into kinetic energy with the $\eta_e < 1$ efficiency factor. Introducing $v_{ex} = g_o\ I_{sp}/\eta_m$ we find,

$$m_w = \frac{\alpha_w\ g_o\ F}{2\ \eta_T} \times I_{sp}$$

the weight of the power equipment increases with the specific impulse. Since the electric thruster needs both propellant and power supply to operate for the initial total mass of the spacecraft m_o we have,

$$m_o = m_f + m_{po} + m_w = m_f + \left(\frac{F\ \tau_b}{g_o}\right) \times \frac{1}{I_{sp}} + \left(\frac{\alpha_w\ g_o\ F}{2\ \eta_T}\right) \times I_{sp} \tag{6.9}$$

where m_f is the constant final mass delivered after the maneuver.

For a constant delivered thrust F and burning time τ_b the second term in equation (6.9) decreases with $I_{sp} = \eta_m\ v_{ex}/g_o$, whereas the second addition linearly grows with the specific impulse. The amount of required propellant reduces as v_{ex} grows but higher exhaust velocities require heavier power supplies. Therefore, an optimal I_{sp} value for m_o exists, as shown in figure 6.4, and the minimum mass corresponds to,

$$\left(I_{sp}\right)_{\min} = \frac{1}{g_o} \sqrt{\frac{2\ \eta_T\ F\ \tau_b}{\alpha_w}}$$

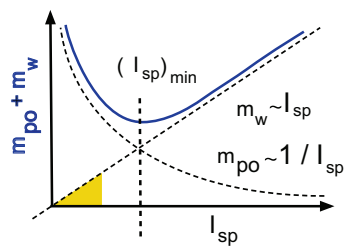

Figure 6.4. The mass $m_{po} + m_w$ of equation (6.9) as a function of I_{sp}.

Next, we study the effect of this optimal value of in the Tsiolkovsky equation (6.2) that relates the increase Δv in the spacecraft velocity and the ratio m_f/m_o between the delivered mass m_f and m_o the initial mass of the system. We have,

$$m_o = m_f + m_{po} + m_w = m_f + m_{po} + \alpha_w \, \eta_T \, P_b$$

and using $P_b = \dot{m}_p \, v_{ex}^2/2$ and $\dot{m}_p = m_p/\tau_b$ then,

$$m_o = m_f + m_{po} + \alpha_w \, \eta_T \, \frac{m_{po} \, v_{ex}^2}{2 \, \tau_b}$$

The ratio $u_b = (2 \, \tau_b/\alpha_w \, \eta_T)^{1/2}$ has the physical units of a velocity and we can write,

$$m_o - m_f = m_{po} \left[1 + \frac{v_{ex}^2}{u_b^2} \right] \quad \text{and,} \quad m_{po} = \frac{m_o - m_f}{1 + (v_{ex}/u_b)^2} \tag{6.10}$$

The mass of the electric power equipment is also,

$$m_w = \alpha_w \, \eta_T \, P_b = \alpha_w \, \eta_T \, \frac{m_{po} \, v_{ex}^2}{2 \, \tau_b}$$

and using the previous expression for m_{po} it can be cast as,

$$m_w = \alpha_w \, \eta_T \frac{v_{ex}^2}{2 \, \tau_b} \, \frac{m_o - m_f}{1 + (v_{ex}/u_b)^2} = \left(\frac{v_{ex}}{u_b} \right)^2 \frac{m_o - m_f}{1 + (v_{ex}/u_b)^2}$$

Finally we obtain,

$$m_w = \frac{m_o - m_f}{1 + (u_b/v_{ex})^2} \tag{6.11}$$

Equation (6.11) can be combined with equation (6.2) where the final mass is $m_f + m_w$ to incorporate the power equipment,

$$\exp\left(\frac{\Delta v}{v_{ex}} \right) = \frac{m_o}{m_f + m_w} = \frac{m_o \, (1 + u_b^2/v_{ex}^2)}{m_o + m_f \, (u_b^2/v_{ex}^2)} = \frac{(1 + v_{ex}^2/u_b^2)}{v_{ex}^2/u_b^2 + m_f/m_o}$$

and finally we can write,

$$\frac{\Delta v}{u_b} = \left(\frac{v_{ex}}{u_b} \right) \ln \left[\frac{(1 + v_{ex}^2/u_b^2)}{v_{ex}^2/u_b^2 + m_f/m_o} \right] \tag{6.12}$$

This expression relates the increments in the spacecraft speed Δv normalized to the characteristic speed $u_b = (2 \, \tau_b/\alpha_w \, \eta_T)^{1/2}$ with scaled exhaust speed v_{ex}/u_b and the ratio between the final m_f and initial m_o masses of the system. The characteristics of the electric power equipment is incorporated in u_b through the coefficient α_w in table 6.4 as well as the total efficiency η_T of the thruster.

Equation (6.12) is represented in figure 6.5 as a function of the normalized exhaust velocity v_{ex}/u_b for different $r = m_f/m_o$ mass ratios. The increments Δv are

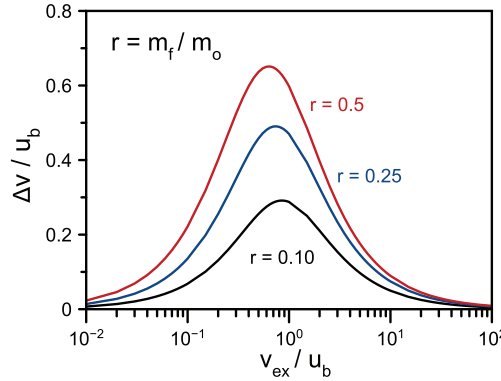

Figure 6.5. Normalized increments $\Delta v/u_b$ (equation 6.12) as a function of v_{ex}/u_b for different $m_r = m_f/m_o$ values.

not equally distributed and it is desirable to operate close to $v_{ex}/u_b \sim 1$ in the vicinity of the sharp maxima. This ratio requires a $\tau_b \sim$ 13 days burning time for a thruster with $\eta_T \sim 0.5$ (see figure 6.3) and propellant exhaust velocity of $v_{ex} \sim 20$ km s^{-1} and $\alpha_w \sim 225$ W kg^{-1} (see table 6.4).

Consequently, the efficient use of electric thrusters requires long times of operation to maximize the low thrust delivered and the need for power equipment that is an integral part of the propulsive system.

6.6 Classification of electric thrusters

The scheme of table 6.5 shows the electric thrusters can be roughly classified in accordance with the physical principle employed for the acceleration of propellant as *electrothermal*, *electrostatic* and *electromagnetic*.

When the working principle of the thruster is the acceleration of a plasma stream, the system usually needs at least one cathode to provide electrons for the ionization of the neutral gas and also for the space charge neutralization of the ion beam [8] (see section 3.4.3). Different electrons sources have been employed, such as thermionic electron emitters or dispenser cathodes, but hollow cathodes are today a standard choice for space applications [7].

The *hollow cathodes* produce the fractional ionization of neutral gas flow using thermionic electrons from a low work function electrode called *insert*, which is heated by an electric current. The plasma is produced by a DC electric discharge at its exit section and it can be seen in operation in the photographs of figures 6.7–6.11. This element is the electron emitting-cathode indicated in the schematic diagrams 6.8, 6.10 and 6.12 of plasma thrusters.

6.6.1 Electrothermal

The *electrothermal* propulsion makes use of an electric current to increase the temperature of the propellant gas by ohmic heating and/or electron-neutral collisions. The kinetic energy of molecules becomes higher and thrust is delivered

Table 6.5. Non-exhaustive classification of EP thrusters where m_a and m_i are, respectively, the masses of molecule and ion. The electric potential is ϕ, the neutral gas or ion temperature is T and J the electric current density. The acronyms are: ECR, electron cyclotron resonance thruster; GIE, gridded ion engine; FEEP, field emission electric propulsion; HET, Hall effect thruster, HEMPT, highly efficient multistage plasma thruster. The applied-field (AF) and self-field (SF) are variants of the magnetoplasmadynamic MPD thruster.

Physical principle			Thruster
Electrothermal	$v_{ex} \sim \sqrt{\frac{T}{m_a}}$	Solid nozzle	Arcjet Resistojet
		Magnetic nozzle	Helicon ECR
Electrostatic	$v_{ex} \sim \sqrt{\frac{2e\phi}{m_i}}$	Externally applied electric field	GIE Colloid FEEP
		Self-consistent electric field	HET HEMPT Multi-Cusp
Electromagnetic	$v_{ex} \sim \frac{J}{\dot{m}}$	Steady plasma flow	AF-MPD SF-MPD
		Unsteady plasma flow	Pulsed plasma

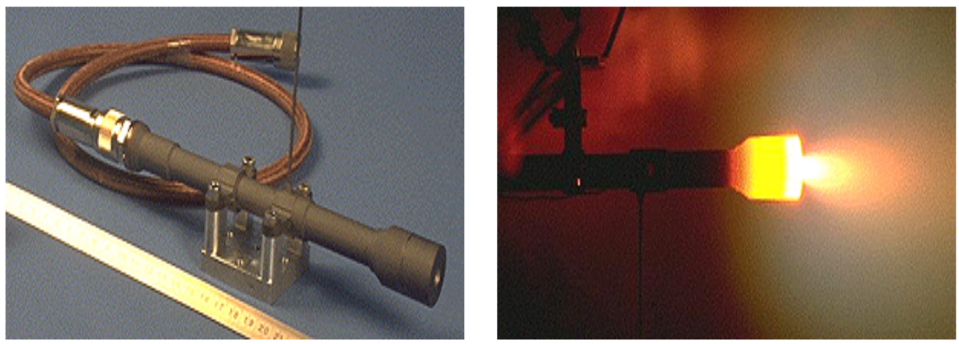

Figure 6.6. The ARTUS-IM3 arcjet on the left and operating into a vacuum chamber on the right picture. (Courtesy Institute of Space Systems, Sttutgart University, Germany.)

to the spacecraft by the expansion through a solid nozzle of this hot neutral gas, usually with a low ionization degree.

The *resistojet* makes use of a resistor to heat the gas and this energy transfer mechanism has a low efficiency, leading to reduced specific impulses of $I_{sp} \sim 100$–300 s in table 6.3, below the limit of figure 6.3 for chemical propulsion.

In the *arcjet* thruster shown in figure 6.6 the heating electric current flows through the propellant and collisions of electrons with neutral gas atoms increase the gas

temperature. The energy transfer requires elevated mass flow rates to increase the electron-neutral ν_{ea} collision frequencies which give $I_{sp} \sim 500$ s, close to the limit of figure 6.3.

Microwave and radio-frequency plasma thrusters (Helicon and electron cyclotron resonance, ECR in table 6.5) are currently included in this categories and are still the subject of study [3]. Different physical mechanisms (helicon wave, electron cyclotron resonance, etc) transfer the energy of an electromagnetic wave to the plasma electrons to increment their kinetic energy and therefore the ionization rate of the propellant gas. Since the motion of charged particles can be restricted along the magnetic field lines, the imparted momentum increases when plasma jet expands through a *magnetic nozzle* configuration [9].

These microwave and RF thrusters essentially rely on the ambipolar electric field introduced in section 3.2.3 to drive the ions that deliver thrust. The advantage is the absence of plasma exposed electrodes and in the case of ECR no cathode is needed to ionize the neutral gas. Therefore, the erosion and wearing of thruster materials is much lower compared with resistojets and arcjets.

6.6.2 Electrostatic

The *electrostatic* thrusters make use of electric power to ionize the propellant neutral gas to produce an electron–ion plasma and momentum is directly imparted to heavy ions by a stationary electric field. As shown in equation (6.6), ions can reach high velocities moving in the field produced by electrodes (usually metallic grids) connected to high voltage power supplies.

In the *gridded ion engines* (GIE, also called Kaufman thrusters) of figure 6.7 the electrons from a cathode placed inside the discharge produce the impact ionization of the propellant gas atoms. Its longitudinal cross sectional diagram of figure 6.8 illustrates the steady state operation of this plasma thruster.

A primary plasma is produced inside the discharge chamber by the electron impact ionization of the propellant neutral gas by free electrons from a hollow

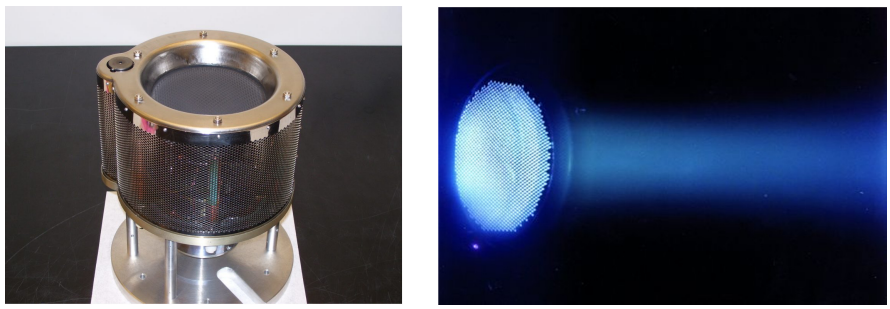

Figure 6.7. The 10 cm diameter T5 ion engine employed in the GOCE mission (left) and this thruster operating in a vacuum tank on the right side. (Courtesy QinetiQ Ltd.) The hollow cathode exit section is the small circle on its surface on the left and in the photograph of the thruster operation on the right, is the small bright blue dot below.

cathode. These are also confined by the magnetic field lines configuration inside the ionization chamber to increase the ionization rate of the neutral gas.

Two grids first extract and then accelerate these ions to high speeds modulated by the electric potential of the acceleration grid of figure 6.8. An additional electron-emitting cathode disposed past the grids provides electrons to neutralize the ion outflow, as was discussed in section 3.4.2. The third external (decelerating) grid is biased at a negative potential to prevent the electrons from the neutralizer cathode moving towards the thruster, since this is a failure mechanism that deteriorates the grids.

The primary plasma production, ion acceleration and space charge neutralization are independent processes in GIE thrusters. Their specific impulses are in the order of $I_{sp} \sim 3000$ s in table 6.3 and deliver $F = 0.001$–1.0 N impulses.

These are regulated by the electric voltage applied to the acceleration grid. The GIE is a mature technology that has been successfully employed in space [1] in the GOCE mission in Earth orbit or the deep space Beppi-Colombo mission to Mercury.

Other thrusters mentioned in table 6.3 make use of similar schemes where electrodes are connected to high voltages. Highly charged micro-droplets of polar liquids accelerated are under kV-range voltage drops are employed by colloid thrusters to impart thrust.

Similarly, the *field emission electric propulsion* (FEEP) produces the electric field ionization of a liquid metal (cesium, indium or mercury) and ions are later accelerated by an externally imposed strong electric field. The advantage is their small size and low power consumption that make them suitable for micro-satellite propulsion and precision motions since they deliver thrusts in the 1–100 μN range with high specific impulses, as indicated in figure 6.3.

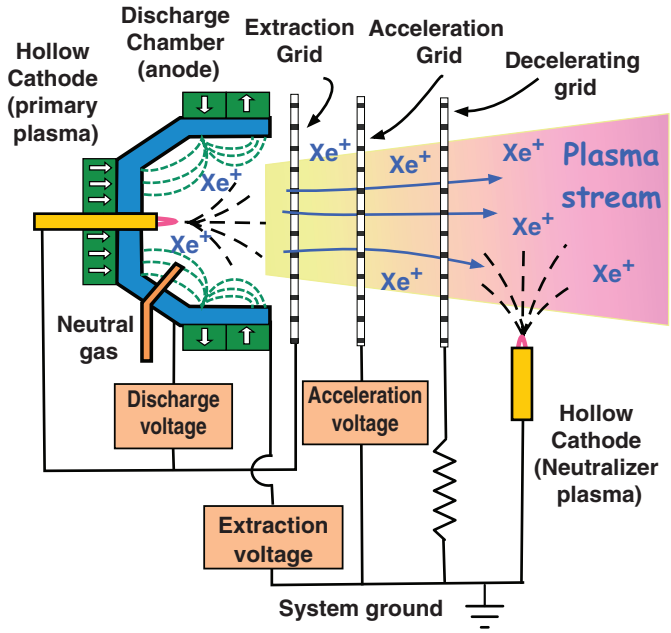

Figure 6.8. Schematic diagram of a gridded ion engine (GIE) as in figure 6.7. The polarity of permanent magnets in green is indicated by the arrows.

Figure 6.9. The Hall effect thruster PPS 1340-E on the left and operating in a vacuum tank in the right photograph. (Courtesy Safran-Snecma.) The hollow cathode is the cylinder attached to the equipment at its upper left and in operation is the bright dot of the right photograph.

The non-equilibrium discharge plasmas can develop internal self-consistent electric fields that can accelerate ions to velocities well over the limit for chemical propulsion indicated in figure 6.2(b). The *Hall effect thruster* (HET) (also called *closed-drift* thruster) of figure 6.9 and the *highly efficient multistage plasma thruster* (HEMPT) shown in figure 6.11 make use of this principle.

The cross sectional scheme of the HET thruster along its longitudinal direction is shown in figure 6.10. The gridless HET has a cylindrical ring shaped ionization chamber usually made of non conductive materials[2] with an annular anode place at its closed end. A radial magnetic field inside is generated by a first pole configuration about the central axis of the system. The second counter-pole magnet surrounds the ionization chamber on the outside.

The only cathode in the Hall thruster is located outside the plasma chamber and is connected to a positive high voltage with respect to the anode. Electrons from this cathode produce the ionization of the propellant neutral gas and also the neutralization of the ion beam. The propellant gas is injected at the back end of the anode and is ionized within the annular ceramic channel. The emitted electrons spread in two directions, moving inwards to the ionization chamber and also along the direction of the plasma beam for space-charge neutralization.

The intensity of radial magnetic field makes the electron Larmor radius smaller than the dimensions of the ionization channel. Their axial motion is inhibited as they move towards the anode since they must cross this intense radial magnetic field formed at the open section of the plasma chamber.

A self-consistent axial electric field develops at the exit section of the ceramic channel since the cathode bias voltage drops along the axial direction where the electrons are trapped by this *magnetic barrier*. This intense electric field accelerates the ions up to speeds of 20–40 km s^{-1} that are non-magnetized because of their heavier mass. This combination of the axial electric field $\boldsymbol{E}$ and radial magnetic field $\boldsymbol{B}$

[2] The discharge chamber is made of metallic materials in the variant of HET called *thruster with anode layer* (TAL), which has a shorter ionization chamber.

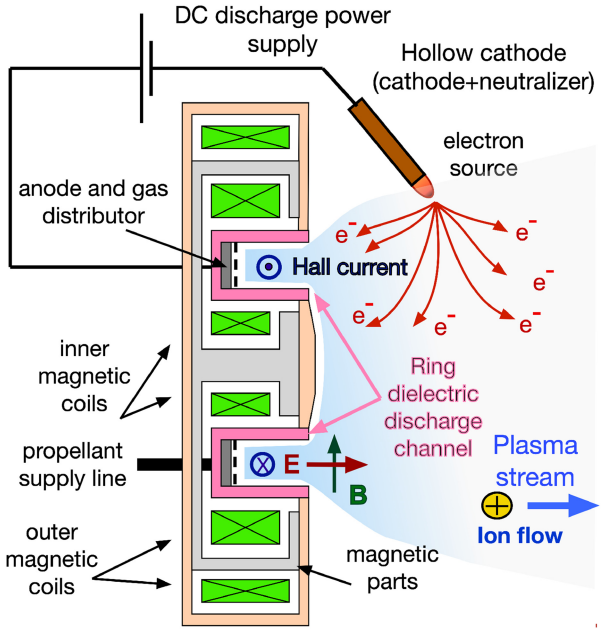

Figure 6.10. Schematic diagram of a Hall effect thruster (HET) as in figure 6.9.

produces an annular Hall current in the $\boldsymbol{E} \times \boldsymbol{B}$ direction that can be seen in figure 6.9, confines the plasma and enhances the ionization rate, as the electrons drift circularly within the annular plasma chamber. Figures 6.7 and 6.9 show the lower divergence HET plasma streams compared with GIE where the ion motion is better focused.

This basic scheme is similar for all different HET configurations and a number of satellites have been equipped with them for in-orbit operation and station keeping [1]. They have a wide range of $F\sim$ 0.01–1 N with specific impulses of $I_{sp}\sim$ 1500 s.

The HEMPT thruster can be considered one of the multi-cusped field thruster category also mentioned in table 6.3, and its cross sectional diagram is shown in figure 6.11. It has a cylindrical discharge chamber made of a non-conductive material with the electron source placed in front of its open side, as in the HET designs. The anode is placed at the closed back end of the ionization chamber on the external surface of which ring shaped permanent magnets with alternate polarities are mounted. One or more annular electrodes are successively distributed longitudinally over the surface of the plasma chamber.

The plasma is produced by biasing the back anode with respect to the external cathode, which provides electrons for neutral gas ionization and neutralization of the ion beam. Electron confinement by the longitudinal magnetic field along the axis of symmetry increases the electron impact ionization rate in the chamber. The ions are accelerated by the multistage electric field established by biasing the electrodes with electric potentials of increasing values between the anode and the cathode potentials.

The divergence of the HEMPT plasma stream is also higher than in GIE as shown in photograph 6.11, and its specific impulses are $I_{sp}\sim$ 1500–3000 s with

Figure 6.11. The HEMPT plasma thruster at the left and operating into a vacuum tank in the right picture. (Courtesy of Thales Group.) The hollow cathode is placed at the upper right of the equipment and it is the bright dot in photograph of the thruster operation.

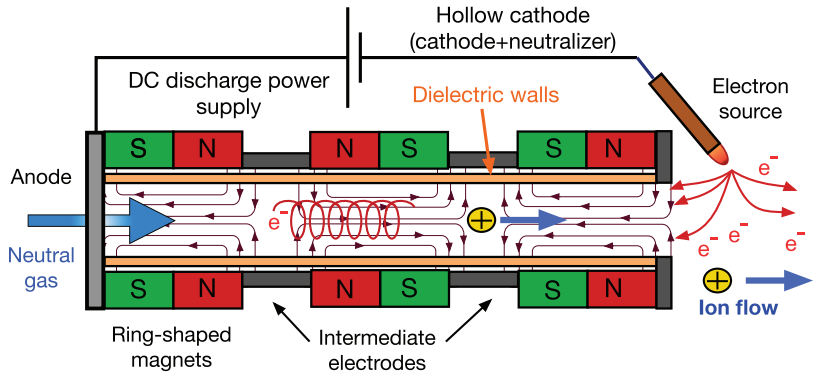

Figure 6.12. Schematic diagram of the HEMPT plasma thruster of figure 6.11.

$F \sim 0.04$–0.1 N impulses. This thruster has reached an important level of development but it has not been tested in orbit so far.

6.6.3 Electromagnetic

The propellant gas is also ionized in the *electromagnetic* propulsion and this plasma is accelerated by the interaction of current flowing through with steady or pulsed electric and magnetic fields established by the currents themselves and/or external means.

These promising and complex devices that are still a subject of research deliver high thrusts ($F \sim$ 0.5–50 N) with specific impulses in the range of 10^3–10^4 s. Their drawback is their large electric power consumption, in the range of megawatts, and their short lifetime by the degradation and evaporation of materials.

In the self-field magnetoplasmadynamic thruster (SF-MPD in table 6.5) a high discharge current $\boldsymbol{j}$ is established between two concentric electrodes. The cathode is disposed along the center line and the propellant flows parallel, whereas $\boldsymbol{j}$ is along in the radial direction. The magnetic Lorentz force $\boldsymbol{F} = \boldsymbol{j} \times \boldsymbol{B}$ resulting from the self-produced magnetic field $\boldsymbol{B}$ in the azimuthal direction accelerates the plasma stream to high velocities.

The applied-field (AF-MPD) thrusters have coils surrounding the thruster to produce an additional magnetic field parallel to the plasma chamber. This applied magnetic field affects the physical processes in the thruster discharge chamber and also the diverging field lines in the plasma expansion region have a geometry similar to a *magnetic nozzle*. Then, the plasma becomes confined along the radial direction and its expansion contributes to the thrust.

6.7 Commentaries and further reading

This chapter is an introduction and not a systematic account of all propulsive systems that use electrical energy. The field is rapidly evolving and new ideas appear constantly. For more information, the interested reader is referred the comprehensive reviews [3, 10] and [11], that offer an excellent up-to-date view of the current state of this technology, as well as [12] and [13]. The book [7] contains an excellent introduction to electric propulsion, specifically to ion engines and Hall thrusters and is more up to date than the classic book [14]. An overview of thermal arcjet thrusters is in the review paper [15].

The electron sources are crucial for electric propulsion systems, the hollow cathodes are today a standard for space applications and are discussed in chapter 6 of reference [7]. Chapter 5 of the book [8] discusses the ion beam neutralization issues. Magnetic nozzles are mainly a subject of research so far and their physical models are complex; reference [9] is a comprehensive review in the context of ECR and Helicon plasma thrusters.

References

[1] List of spacecrafts with electric propulsion. Wikipedia https://en.wikipedia.org/wiki/List_of_spacecraft_with_electric_propulsion accessed on May 22, 2020

[2] Dudeck M, Doveil F, Arcis N and Zurbach S 2012 Plasma propulsion for geostationary satellites for telecommunication and interplanetary missions *IOP Conf. Ser.: Mater. Sci. Eng.* **29** 012010

[3] Mazouffre S 2016 Electric propulsion for satellites and spacecraft: established technologies and novel approaches *Plasma Sour. Sci. Technol.* **25** 1–27

[4] Sutton G P and Biblarz O 2001 *Rocket Propulsion Elements* (New York: Wiley)

[5] Boch E 2017 The HEMPT NG *Proc. of the Electric Propulsion, Innovation & Competitiveness Workshop (Madrid, Spain)*

[6] Koch N *et al* 2011 The HEMPT concept. A survey on theoretical considerations and experimental evidences *Proc. of the 32th Int. Electric Propulsion Conf. (Weisbaden, Germany)* IEPC paper 2011-236

[7] Goebel D M and Katz I 2008 *Fundamentals of Electric Propulsion. Ion and Hall Thrusters* (Hoboken, NJ: Wiley)

[8] Humphries S 2013 *Charged Particle Beams* 2nd edn (New York: Dover)
[9] Takahasi K 2019 Helicon-type radiofrequency plasma thrusters and magnetic plasma nozzles *Rev. Mod. Plasma Phys.* **3** 1–61
[10] Levchenko I, Xu S, Mazouffre S, Lev D, Pedrini D, Goebel D, Garrigues L, Taccogna F and Bazaka K 2020 Perspectives, frontiers, and new horizons for plasma-based space electric propulsion *Phys. Plasmas* **27** 020601
[11] Jahn R G and Choueiri E Y 2002 Electric propulsion *Encyclopedia of Physical Science and Technology* ed R A Mayers vol 5 3rd edn (Cambridge MA: Academic)
[12] Charles C 2009 Plasmas for spacecraft propulsion *J. Phys. D: Appl. Phys.* **42** 163001
[13] Ahedo E 2011 Plasmas for space propulsion *Plasma Phys. Control. Fusion* **53** 124037
[14] Jahn R G 2006 *Physics of Electric Propulsion* 2nd edn (New York: Dover)
[15] Wollenhaupt B, Le Q H and Herdrich G 2018 Overview of thermal arcjet thruster development *Aircr. Eng. Aerosp. Tech.* **90** 353–68